Development of nanostructure materials and architecture for high performance Li-rechargeable batteries with ultrafast charge rate

Principle Investigator: Li Lu, Professor Dr.

Department of Mechanical Engineering

National University of Singapore

AFOSR/AOARD RD: FA2386-10-1-4013

25 Nov 2009 ~ 24 Feb 2011

Report Documentation Page

Form Approved
OMB No. 0704-0188

1. REPORT DATE	2. REPORT TYPE	3. DATES COVERED
22 APR 2011	**Final**	**25-11-2010 to 24-02-2011**

4. TITLE AND SUBTITLE
Li-rechargeable batteries with ultrafast charge rate

5a. CONTRACT NUMBER
FA23861014013

5b. GRANT NUMBER

5c. PROGRAM ELEMENT NUMBER

6. AUTHOR(S)
Liu Lu

5d. PROJECT NUMBER

5e. TASK NUMBER

5f. WORK UNIT NUMBER

7. PERFORMING ORGANIZATION NAME(S) AND ADDRESS(ES)
National University of Singapore,9 Engineering Drive 1,Singapore 117576,Singapore,NA,NA

8. PERFORMING ORGANIZATION REPORT NUMBER
N/A

9. SPONSORING/MONITORING AGENCY NAME(S) AND ADDRESS(ES)
AOARD, UNIT 45002, APO, AP, 96337-5002

10. SPONSOR/MONITOR'S ACRONYM(S)
AOARD

11. SPONSOR/MONITOR'S REPORT NUMBER(S)
AOARD-104013

12. DISTRIBUTION/AVAILABILITY STATEMENT
Approved for public release; distribution unlimited

13. SUPPLEMENTARY NOTES

14. ABSTRACT

Nano sized LiNi0.5-2xRuxMn1.5O4 (x=0, 0.01, 0.03 and 0.05) spinels have been successfully synthesized by polymer assisted method. SEM observation shows that particles? sizes of LiNi0.5-2xRuxMn1.5O4 are around 300 nm. XRD and FTIR measurements prove that all Ru doped samples have phase pure spinel structure with Fd3m space group, while pristine LiNi0.5Mn1.5O4 contains impurity phase (LixNi1-xO). The nano sized LiNi0.5Mn1.5O4 can release 117 mAh. g-1 at 10 C discharge rate; while, the nano sized LiNi0.4Ru0.05Mn1.5O4 can deliver 135 mAh. g-1 at 10 C discharge rate. In 500 cycles 10 C charge/discharge test, the nano sized LiNi0.4Ru0.05Mn1.5O4 can initially deliver near 121 mAh. g-1 and still keep 100 mAh. g-1 at the 500th cycle exhibiting much better cyclic performance than the pristine LiNi0.5Mn1.5O4. It also exhibits excellent cyclic performances when charge/discharged at 10C for 1000 cycles. The great improvements on high rate performances of Ru doped cathodes can be attributed to their higher electronic conductivity and lithium diffusion coefficient, which are achieved through both Ru doping and reduction of particle size.

15. SUBJECT TERMS
lithium ion secondary battery, High Power Generation, Nanostructured materials, Ru doping

16. SECURITY CLASSIFICATION OF:			17. LIMITATION OF ABSTRACT	18. NUMBER OF PAGES	19a. NAME OF RESPONSIBLE PERSON
a. REPORT	b. ABSTRACT	c. THIS PAGE			
unclassified	**unclassified**	**unclassified**	**Same as Report (SAR)**	**29**	

1. Introduction

Since the first introduction of $Li_xC_6/Li_{1-x}CoO_2$ rechargeable battery by Sony Corporation in 1991, the application of lithium-ion batteries for portable electronic devices has been growing at a very high rate. Recently, the imperative of tackling environmental pollution and exhaustion of fossil fuel reserves has rendered the electric vehicles (EVs) of greater importance than ever before. In addition to civil applications, lithium batteries are also becoming attractive to defense and aerospace industrials due to their good prospect of high power and high energy density. However, the power density of the conventional lithium-ion batteries is generally low due to the extensive polarization at high current densities. This in turn, has drawn great interests to develop new cathode materials with much better high-rate performances than that of conventional $LiCoO_2$.[1-6]

$LiMn_2O_4$ has been considered as a promising alternative to replace $LiCoO_2$. It has a face centered cubic spinel structure with Li and Mn occupying tetrahedral and octahedral sites, respectively. However, the presence of Mn^{3+} ion ($3d^4$) in the $LiMn_2O_4$ leads to a well-known Jahn-Teller (J-T) distortion causing severe structural instability.[6-7] Moreover, high concentration of Mn^{3+} on surfaces of particles makes electrode vulnerable to acid attack in the electrolyte, which further deteriorates capacity retention.[8-9] To address this problem, mono-, di-, and trivalent cation substitutions for Mn^{3+} have been used to raise the average valence of Mn ions.[10-16] Among these newly develop spinels $LiM_xMn_{2-x}O_4$ (M=Ni, Fe, Co, Cr and Cu),

$LiNi_{0.5}Mn_{1.5}O_4$ has received great attention owing to its significant reversible capacity at about 4.7 V vs. Li/Li^+.[17-19] Such high operation voltage of $LiNi_{0.5}Mn_{1.5}O_4$ can open up new prospects for the next generation of lithium batteries with higher energy and power densities.[20]

$LiNi_{0.5}Mn_{1.5}O_4$ has been identified to possess two possible lattice structures depending on the synthesis conditions. One is the face centered spinel ($Fd\bar{3}m$), and the other is primitive simple cubic ($P4_332$).[18,21] For the $LiNi_{0.5}Mn_{1.5}O_4$ with space group $Fd\bar{3}m$, its basic structure is formed by oxygen ions in a cubic closed packed way occupying 32e positions. The Li ions are located at 8a tetrahedral sites, and Ni and Mn are randomly distributed on the 16d octadedral sites. The synthesis of the $LiNi_{0.5}Mn_{1.5}O_4$ with space group $Fd\bar{3}m$ is usually carried out at a temperature higher than 750 ºC. For the $LiNi_{0.5}Mn_{1.5}O_4$ with space group $P4_332$, the oxygen ions occupy the 8c and 24e positions, while Li ions occupy 8c sites. The Mn ions and Ni ions occupy 12d and 4a octahedral sites, respectively. The formation of the $LiNi_{0.5}Mn_{1.5}O_4$ with space group $P4_332$ is usually achieved by annealing $LiNi_{0.5}Mn_{1.5}O_4$ ($Fd\bar{3}m$) at 700 ºC.[22] There are few Mn^{3+} exist in the $LiNi_{0.5}Mn_{1.5}O_4$ ($Fd\bar{3}m$) due to loss of oxygen at high temperature treatment (higher than 750 ºC). However, many research work has proved that the electrochemical performance of the $LiNi_{0.5}Mn_{1.5}O_4$ ($Fd\bar{3}m$) is better than that of the $LiNi_{0.5}Mn_{1.5}O_4$ ($P4_332$). Such difference can be attributed to higher conductivity of the $LiNi_{0.5}Mn_{1.5}O_4$ ($Fd\bar{3}m$) and structure transformation of the the $LiNi_{0.5}Mn_{1.5}O_4$ ($P4_332$) during operation. Therefore, the $LiNi_{0.5}Mn_{1.5}O_4$ ($Fd\bar{3}m$) is more attractive for battery applications. The average

valence of Mn in the $LiNi_{0.5}Mn_{1.5}O_4$ ($Fd\bar{3}m$) is nearly 4, which could avoid the J-T structural distortion and acid attack from the electrolyte, thus $LiNi_{0.5}Mn_{1.5}O_4$ exhibits significantly improved cyclic performance compared to $LiMn_2O_4$ at modest current rates.[21,23,24]

Although it possesses many advantages, $LiNi_{0.5}Mn_{1.5}O_4$ still encounters many obstacles for high rate applications including low accessible capacity and poor cyclic performance due mainly to reaction with electrolyte, existence of $Li_xNi_{1-x}O$ impurity and formation of three cubic phases during cycling ($P4_332$ structure). To overcome these difficulties extensive work has been done. Surface coatings with ZnO, SiO_2, and Bi_2O_3 have been proposed to enhance stability of electrodes.[25-27] And these research results have implied that the detrimental effect of HF in electrolyte towards the $LiNi_{0.5}Mn_{1.5}O_4$ cathode can be suppressed using proper oxides coating, and improved capacity retention has been obtained through particles' surface coating. Cationic doping using 3d transition metals (Cr, Co, Fe and Cu) have also been adopted to eliminate $Li_xNi_{1-x}O$ and stabilize its crystal structure.[28-33] Through doping foreign proper 3d transition metal ions, the formation of undesired $Li_xNi_{1-x}O$ can be suppressed and the desired $Fd\bar{3}m$ structure is maintained.

Relative low conductivity of the $LiNi_{0.5}Mn_{1.5}O_4$ is another main drawback restricting its high-rate performance. As a result of the low conductivity, Li^+ ions are easily piled-up on surfaces of particles forming $Li_{2-\delta}Ni_{0.5}Mn_{1.5}O_4$ during high-rate discharge, in which a large amount of Mn^{3+} ions present to keep charge neutrality. Consequently, detrimental effects caused by the high Mn^{3+} concentration on the

surface of the particles gradually deteriorate electrochemical performances by pronounced J-T distortion and acid attack from HF.[34] To enhance their conductivity, nanotechnologies have been employed to shorten transportation length of Li^+ ions and electrons. Nano sized $LiNi_{0.5}Mn_{1.5}O_4$ have been successfully synthesized using polymer assisted method, Pechini method, controlled precipitation method and ethylene glycol-assisted method. The results have shown that at high discharge rate of 5 C and 10 C, the accessible capacity of nano sized $LiNi_{0.5}Mn_{1.5}O_4$ can be between 100 and 110 mAh. g^{-1}, and the cyclic performance (below 200 cycles) also can be improved.[35-38] Another strategy often used is to dope the framework with a 3d transition-metal ion to enhance inherent conductivity. Cr doped $LiNi_{0.5}Mn_{1.5}O_4$ has been reported could release nearly 140 mAh. g^{-1} and maintain reversible within 80 cycles,[29] however this amazing result has not been repeated by other groups doping Cr. Co doped $LiNi_{0.5}Mn_{1.5}O_4$ has shown a promising discharge capacity of nearly 120 mAh .g^{-1} and superior capacity retention at 3.5 C.[31] Fe doped $LiNi_{0.5}Mn_{1.5}O_4$ also has been reported that it could deliver nearly 110 mAh. g^{-1} with improved cyclic performance at 10C.[32] All these achievements are reported due to either improvement on lithium diffusion coefficient or decrease in resistance after doping 3d transitional metals. However, only few reports have been published regarding doping 4d transition metals such as Ru into $LiNi_{0.5}Mn_{1.5}O_4$.[39-40] In comparison with 3d orbitals, the 4d orbitals with larger radius of the second row transition metal ions overlapping with the 2p orbitals of oxygen favors wider conduction bands.[41] Many oxides containing 4d transition metal ions such as $BaMoO_3$, $SrMoO_3$, $SrRuO_3$,

$CaRuO_3$, and $SrTi_{1-x}Ru_xO_3$ exhibit superior conductivity.[41-42] Especially, RuO_2 and Li_2RuO_3 are promising electrode materials for high power lithium ion batteries due to their good conductivity.[43-44] In previous research, our group successfully synthesized micron sized $LiNi_{0.4}Ru_{0.05}Mn_{1.5}O_4$ and $Li_{1.1}Ni_{0.35}Ru_{0.05}Mn_{1.5}O_4$ exhibiting excellent rate capabilities and cyclic performances.[39] A recent research work attempted to substitute Mn with Ru in $LiNi_{0.5}Mn_{1.5}O_4$, however two phases present in the final product.[40]

According to our previous research results, Ru doping in to $LiNi_{0.5}Mn_{1.5}O_4$ can greatly enhance the electronic conductivity as shown by $Li_{1.1}Ni_{0.35}Ru_{0.05}Mn_{1.5}O_4$ and $LiNi_{0.4}Ru_{0.05}Mn_{1.5}O_4$. While, further investigations imply that the $LiNi_{0.4}Ru_{0.05}Mn_{1.5}O_4$ with some crystal defects at octahedral sites could enable faster lithium ion transportation process leading to much better high rate performance compared with the $Li_{1.1}Ni_{0.35}Ru_{0.05}Mn_{1.5}O_4$. In order to obtain larger capacity and better cyclic performance at high rates, we combine the Ru doping method and nanotechnology to produce nano sized $LiNi_{0.5-2x}Ru_xMn_{1.5}O_4$ (x=0, 0.01, 0.03 and 0.05) spinel cathodes. In this research project, we systematically investigate the composition, morphology, structure, lithium diffusivity and high-rate performances of the nano sized $LiNi_{0.5-2x}Ru_xMn_{1.5}O_4$ (x=0, 0.01, 0.03 and 0.05) spinels. The results provide clear evidence that both the Ru-doping and reduction of particles' size can effectively improve the charge transportation properties of the spinel cathodes, and maintain structural stability by preventing the present of detrimental Mn^{3+} ions at high

current densities, which shall provide novel hints to develop next generation lithium ion batteries with desirable high rate performances.

2. Experiment Procedure

Materials Design

To maintain the existed superiority of $LiNi_{0.5}Mn_{1.5}O_4$ such as high operation voltage (4.7 V vs. Li/Li^+) and stability during charge/discharge at modest current rate, doping experiments should not dramatically alter the original spinel structure. A perfect cubic spinel structure can be formulated as AB_2O_4, the doped new compound should generally keep this formula with slight deviations to keep charge neutrality within the structure. Firstly, both Ni^{2+} and Mn^{4+} occupy octahedral sites in $LiNi_{0.5}Mn_{1.5}O_4$ making them both the possible doping targets. The effective ionic radius of octahedrally coordinated Mn^{4+} and Ni^{2+} is 0.53 Å and 0.69 Å, respectively. While the effective ionic radius of octahedrally coordinated Ru^{4+} is 0.62 Å.[45] It is obviously that Ni^{2+} would be easier to be substituted by these 4d transition metal ions due to similar ionic radius. Both our previous research and a recent report have confirmed that using Ru replace Mn in the $LiNi_{0.5}Mn_{1.5}O_4$ results in formation of two phases,[39-40] which is possibly due to the unmatched ionic radius. Secondly, compound formula needs to be modified to maintain charge neutrality and without introduce undesired Mn^{3+} ions; therefore some defects will be introduced into new formula. Thirdly, since Ni is the major electrons contributor in $LiNi_{0.5}Mn_{1.5}O_4$, the doping content should be small otherwise the capacity will be dramatically reduced. In

addition, 4d transitional metals are expensive which also requires the doping content should be controlled in a reasonable level. Taking all these factors into consideration, a general formula of $LiNi_{0.5-2x}Ru_xMn_{1.5}O_4$ (x=0, 0.01, 0.03 and 0.05) is designed. Ru doped in to the spinel lattice is designed to have a valence state of 4+. To keep charge neutrality, every two Ni^{2+} ions will be substituted by one Ru^{4+} ions leaving one vacancy on octahedral site. As described in the introduction, such octahedral vacancy may have positively influence on lithium transportation process.

Materials Preparation.

The nanosized $LiNi_{0.5-2x}Ru_xMn_{1.5}O_4$ samples were prepared using polymer assisted method. Firstly, $LiOOCCH_3.2H_2O$, $Mn(OOCCH_3)_2.4H_2O$, $Ni(OOCCH_3)_2.4H_2O$ and $RuCl_3$ were stoichiometrically mixed with $H_2C_2O_4 \cdot 2H_2O$ and ground in a planetary Restach ball mill for 2 hours to obtain homogeneous mixture; then 40 ml polymer (PEG-400) was added and continue ball milling for 12 hours to obtain grey slurry; finally, the mixture were calcined at 300 ºC for 2 hours followed by firing at 800 ºC for 2 hours to obtain the final products.

Materials characterization

The element proportion of each sample was determined by inductively coupled plasma emission spectrometry (ICP-AES, ICPE 9000 SHIMAZU). Structural and phase analysis were conducted by X-ray diffraction analysis using a XRD-7000 diffractometer (SHIMADZU) with a Cu Kα radiation source (λ=1.5418 Å). Fourier

transform infrared spectra (FTIR) were recorded with KBr pellets with a IRPrestige-21 IR spectrophotometer. Field scanning electron microscopy (Hitachi FESEM-4100) was employed to study the particles' morphology.

Electrochemical tests

Charge and discharge were performed by galvanostatically cycling between 3 and 5 V using a Maccor-4 battery tester. The lithium diffusion coefficient (D_{Li}) were measured by potential intermittent titration technique (PITT) on the batteries using $LiNi_{0.5-2x}Ru_xMn_{1.5}O_4$ (x=0 and 0.05) as cathodes. The Swagelok cells were assembled in argon filled glove box using the Li foil as counter electrode. The cathode was fabricated using 80 wt % active material with 10 wt % Super P, and 10 wt % polyvinylidene difluoride (PVDF) The average loading density of active material is 2.5 mg cm^{-2}. The electrolyte was $LiPF_6$ (1 M) in 1:1 mixture of diethyl carbonate and ethylene carbonate electrolyte.

3. Results and Discussion

Materials Characterization

Figure 1 shows the morphologies of the $LiNi_{0.5-2x}Ru_xMn_{1.5}O_4$ powders synthesized by polymer assisted method. The average particle size is only about 300 nm, which is less than half of the particle size of the $LiNi_{0.5-2x}Ru_xMn_{1.5}O_4$ synthesized by traditional solid state reactions.

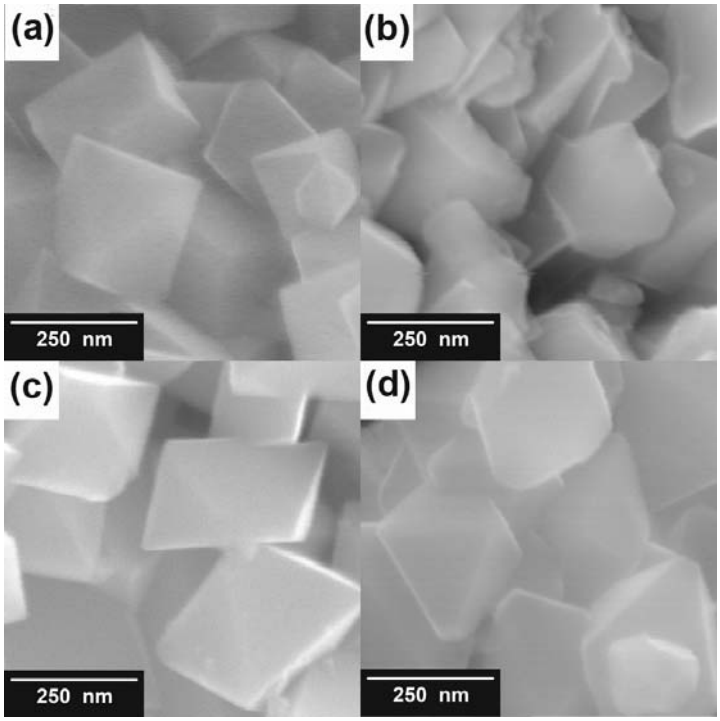

Figure 1. SEM morphology of the $LiNi_{0.5-2x}Ru_xMn_{1.5}O_4$: (a) x=0, (b) x=0.01, (c) x=0.03 and (d) x=0.05.

Table 1. ICP results of $LiNi_{0.5-2x}Ru_xMn_{1.5}O_4$ (x=0, 0.01, 0.03, and 0.05)

Ru content	Li	Ni	Ru	Mn
x=0	0.97	0.5	0	1.5
x=0.01	0.97	0.48	0.01	1.5
x=0.03	0.98	0.44	0.03	1.49
x=0.05	0.98	0.4	0.05	1.5

The elemental ratio of the $LiNi_{0.5-2x}Ru_xMn_{1.5}O_4$ (x=0, 0.01, 0.03 and 0.05) were determined by ICP-AES measurements. The results are shown in table 1. It can be seen from the table that the elemental ratio of Ni, Ru and Mn is basically consistent with designed composition. However, the content of lithium in each sample does not

reach 1, which probably is ascribed to the low sensitive of ICP technique to light metal elements such as lithium. Existence of trace amount of impurity elements may also lead to such deviation. Generally, the Ru doping content is consistent with the designed composition for all products.

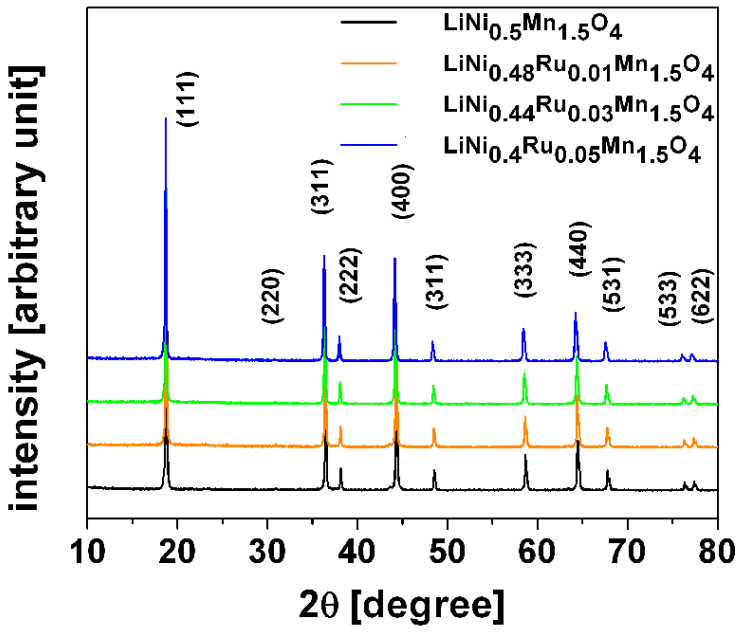

Fig 2. XRD results of the $LiNi_{0.5-2x}Ru_xMn_{1.5}O_4$ (x=0, 0.01, 0.03 and 0.05)

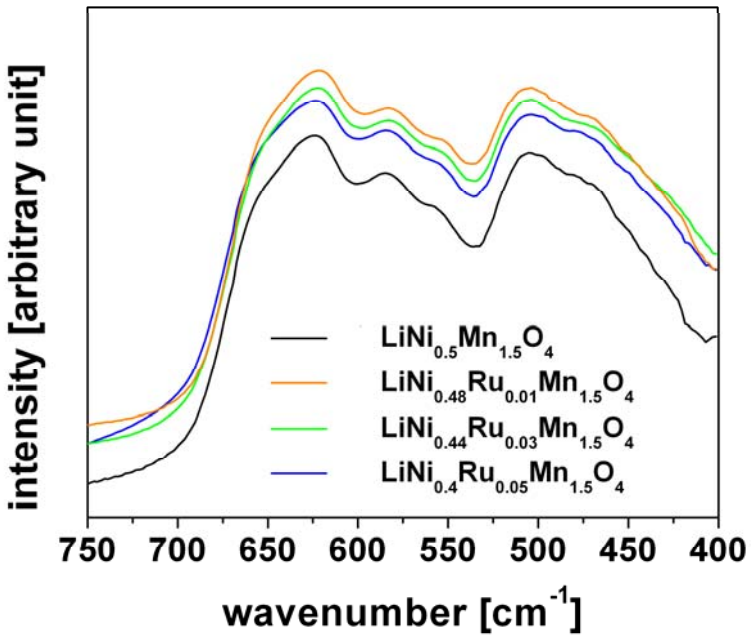

Fig 3. FTIR results of the $LiNi_{0.5-2x}Ru_xMn_{1.5}O_4$ (x=0, 0.01, 0.03 and 0.05)

The XRD profiles of the $LiNi_{0.5-2x}Ru_xMn_{1.5}O_4$ (x=0, 0.01, 0.03 and 0.05) are exhibited in Figure 2. Weak peaks observed at 37.5 °, 45.3 ° and 63.7 ° are due to $Li_xNi_{1-x}O$ impurity in the $LiNi_{0.5}Mn_{1.5}O_4$ sample, which is a common seen byproduct in synthesis of $LiNi_{0.5}Mn_{1.5}O_4$. While, all the Ru-doped samples reveal phase-pure cubic spinel structure without impurity, which is consistent with earlier reports that the cationic doping can suppress the formation of the $Li_xNi_{1-x}O$ and stabilize the spinel crystal structure. The presence of the (220) weak peaks may imply some extent of 'cation mixing' with presences of heavier transition metal ions in the tetrahedral *8a* site instead of Li^+ ions.[35,46-47] There is no clear evidence of the existence of RuO_2 in the final products, which may imply that Ru has been doped in to the spinel structure. The XRD profiles for the four spinels show that all the peaks

fit well to the space group of $Fd\bar{3}m$ implying random mixing of transition metal ions in octahedral *16d* sites. However, the difference of XRD profile between $Fd\bar{3}m$ and $P4_332$ structure is very small. Fourier transform infrared spectra (FTIR) has been proved to be sensitive to the lattice variation (ordered or disordered) of $LiNi_{0.5}Mn_{1.5}O_4$ based cathodes,[32,48] therefore, FTIR measurement was employed to verify the conclusion of XRD test. The FTIR spectra of the $LiNi_{0.5-2x}Ru_xMn_{1.5}O_4$ (x=0, 0.01, 0.03 and 0.05) are shown in Figure 3 exhibiting similar profiles, which implies they all adopt the same crystal structure. The characteristics bands (at around 465 and 430 cm^{-1}) of the cation ordered structure ($P4_332$) were not observed in the spectra of the $LiNi_{0.5-2x}Ru_xMn_{1.5}O_4$ (x=0, 0.01, 0.03 and 0.05). It can be concluded that all these four spinels adopt a cation disordered structure ($Fd\bar{3}m$), which is consistent with the result of XRD analysis.

Electrochemical performances

The charge/discharge profiles of cathodes at low current rate usually can reflect their maximum accessible capacity and theoretical operation voltage plateaus, since very little polarization exists at low rate.

All the nano sized $LiNi_{0.5-2x}Ru_xMn_{1.5}O_4$ (x=0, 0.01, 0.03 and 0.05) are charged/discharged at a low current rate of 0.2 C (29.4 mA. g^{-1}) to examine their operation profiles. Fig 4 a to 4 d displays their charge/discharge profiles at 0.2 C.

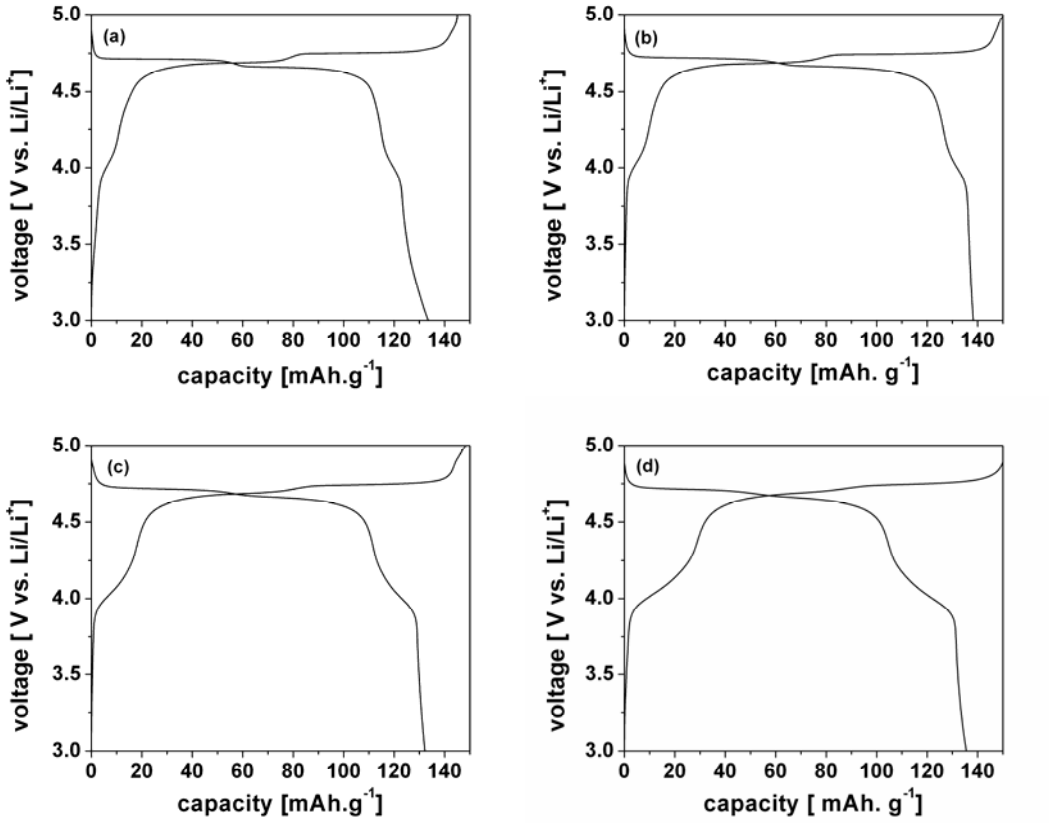

Figure 4. charge/discharge profiles of the $LiNi_{0.5-2x}Ru_xMn_{1.5}O_4$ (x=0, 0.01, 0.03 and 0.05) at 0.2C

The theoretical capacity of $LiNi_{0.5}Mn_{1.5}O_4$ is 147 mAh. g^{-1}. While at 0.2 C, the accessible discharge capacity of as-synthesized $LiNi_{0.5}Mn_{1.5}O_4$ is about 134 mAh. g^{-1} as shown in Figure 4 a, which is consistent with other researchers' results. It can be seen that $LiNi_{0.48}Ru_{0.01}Mn_{1.5}O_4$ can provide the largest capacity of 138 mAh. g^{-1}, while the $LiNi_{0.44}Ru_{0.03}Mn_{1.5}O_4$ and the $LiNi_{0.4}Ru_{0.05}Mn_{1.5}O_4$ can release similar capacity with $LiNi_{0.5}Mn_{1.5}O_4$. Theoretically, reduce of Ni content would lead to decrease in capacity since the $Ni^{2+/4+}$ redox contribute most electrons. However, accessible discharge capacities of all Ru doped cathodes do not show significant difference compared with that of pristine $LiNi_{0.5}Mn_{1.5}O_4$.

Two distinguished discharge plateaus can be identified for the pristine

$LiNi_{0.5}Mn_{1.5}O_4$. The major one is around 4.7 V attributing to $Ni^{2+/4+}$ redox reactions. The smaller one is around 4.0 caused by small amount of $Mn^{3+/4+}$ redox reactions, which is commonly seen in $LiNi_{0.5}Mn_{1.5}O_4$ with $Fd\bar{3}m$ space group. For the pristine $LiNi_{0.5}Mn_{1.5}O_4$, the 4.7 V plateau contributes more than 110 mAh. g^{-1} discharge capacity. While for Ru doped samples, all 4.7 V plateaus shrink due to less Ni^{2+} content. The 4.7 plateaus of the $LiNi_{0.4}Ru_{0.05}Mn_{1.5}O_4$ only contribute less than 100 mAh.g^{-1} discharge capacity respectively. The plateaus around 4.0 V of all Ru doped samples become longer compared with that of the pristine $LiNi_{0.5}Mn_{1.5}O_4$. At this point, it is hard to determine whether additional Mn^{3+} ions are introduced into the $LiNi_{0.4}Ru_{0.05}Mn_{1.5}O_4$, since Reddy et al has proved that $Ru^{4+/5+}$ redox is active in spinel structured $LiMn_{2-x}Ru_xO_4$ and contribute discharge capacity at around 4.2 V.[49] It is also highly possible that $Ru^{4+/5+}$ redox reactions also can work in spinel structured $LiNi_{0.5-2x}Ru_xMn_{1.5}O_4$ resulting in elongation of 4.0 V plateaus.

The galvanostatic curves of the $LiNi_{0.5-2x}Ru_xMn_{1.5}O_4$ (x=0, 0.01, 0.03 and 0.05) are plotted in the form of differential capacities (dQ/dV) and shown through Fig 5a to 5d, which has been widely used to identify the electrochemical redox reactions. Previously obtained charge/discharge curves at the rate of 0.2C was used to generate these dQ/dV curves.

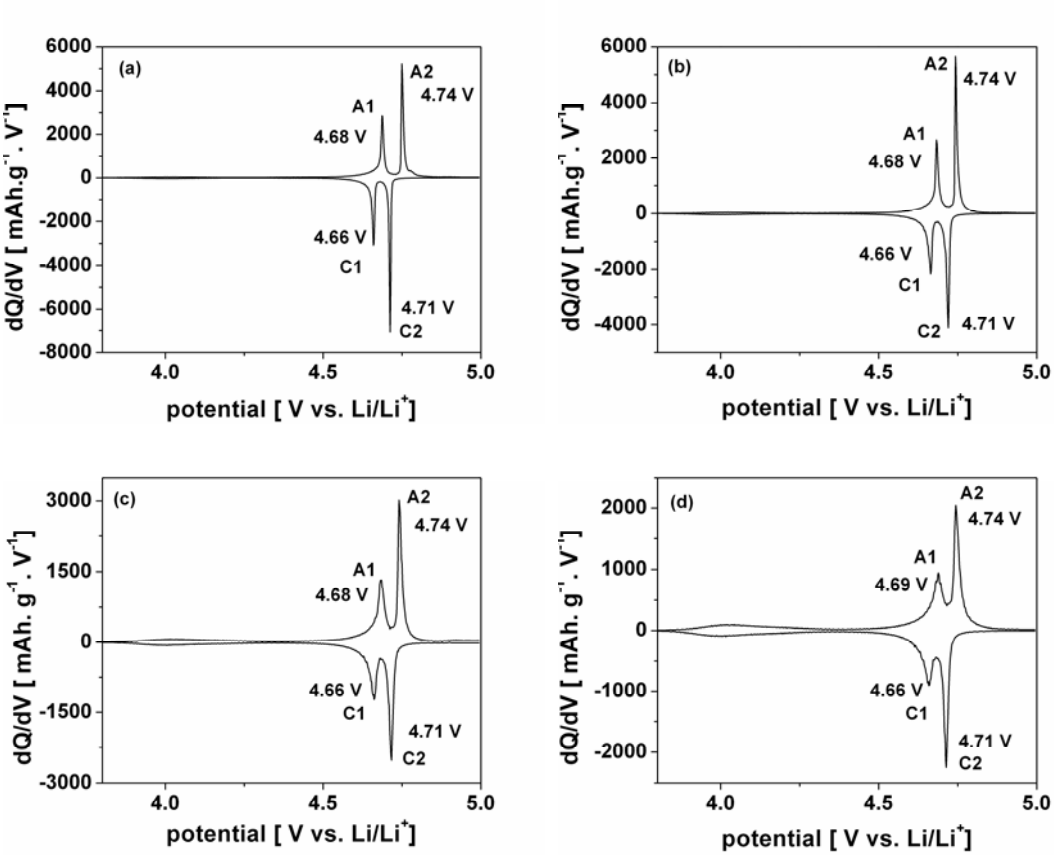

Figure 5. dQ/dV plots of the $LiNi_{0.5-2x}Ru_xMn_{1.5}O_4$ (x=0, 0.01, 0.03 and 0.05)

The dQ/dV curve of the pristine $LiNi_{0.5}Mn_{1.5}O_4$ shows several peaks with increasing voltage, which are ascribed to oxidation of constituents in cathode materials. The peak pairs around .6 V and 4.7 V are known to be contributed by $Ni^{2+/3+}$ and $Ni^{3+/4+}$ redox. Similar peak pairs are also found in the dQ/dV profiles of all Ru doped samples. Interestingly, there is nearly no peak presents at around 4.0 V for the pristine $LiNi_{0.5}Mn_{1.5}O_4$, which can be easily observed on the dQ/dV profiles of $LiNi_{0.5}Mn_{1.5}O_4$ prepared by solid state reactions in our previous research. And it is known that $Mn^{3+/4+}$ is the origin of 4.0 V peaks in $LiNi_{0.5}Mn_{1.5}O_4$. This result implies that polymer assisted method is less prone to generate Mn^{3+} ions in lattice compared

to solid state reactions at 800 ºC. Another interesting phenomenon is that a broad peak pair ranging from 4.0 to 4.3 V appears in all Ru doped samples, and become larger as the Ru content increases. Reddy et al. have observed clear redox peaks of $Ru^{4+/5+}$ in spinel structured $LiMn_{2-x}Ru_xO_4$ between 4.0 and 4.3 V,[49] therefore, the variation of the broad peak pair in this range may provide a hint that $Ru^{4+/5+}$ redox also contributes in charge transportation in $LiNi_{0.5-2x}Ru_xMn_{1.5}O_4$. However, due to trace amount of Ru content and overlap with $Mn^{3+/4+}$ peaks, the effect of $Mn^{3+/4+}$ redox cannot be ruled out.

The potential values of the anodic and cathodic peaks were carefully examined, and the potential values of the anodic peaks (A1 and A2) and cathodic peaks (C1 and C2) of the $LiNi_{0.5-2x}Ru_xMn_{1.5}O_4$ (x=0, 0.01, 0.03 and 0.05) at around 4.7 V are also shown in Fig 5. The potential difference of A1-C1 and A2-C2 can reflect the ease of insertion/extraction Li^+ ions in the spinel structure.[32,50] Unlike the previous results of micron sized $LiNi_{0.5-2x}Ru_xMn_{1.5}O_4$ synthesized by solid state reactions that the potential differences become smaller for the Ru doped samples, there is basically no significant difference can be observed between the $LiNi_{0.5-2x}Ru_xMn_{1.5}O_4$ synthesized by polymer assisted method. This can be attributed to dramatically reduced particles' size (300 nm) yielding from polymer assisted method. As particle size decreases, the distance of Li ions transport from the surface to the core of particle also decreases dramatically so that Li ions are easier to be inserted /extracted in to particles. The effect of reduction of particle size is so pronounced that it is hard to tell the difference between pristine $LiNi_{0.5}Mn_{1.5}O_4$ and Ru doped $LiNi_{0.5}Mn_{1.5}O_4$ from the

dQ/dV plots.

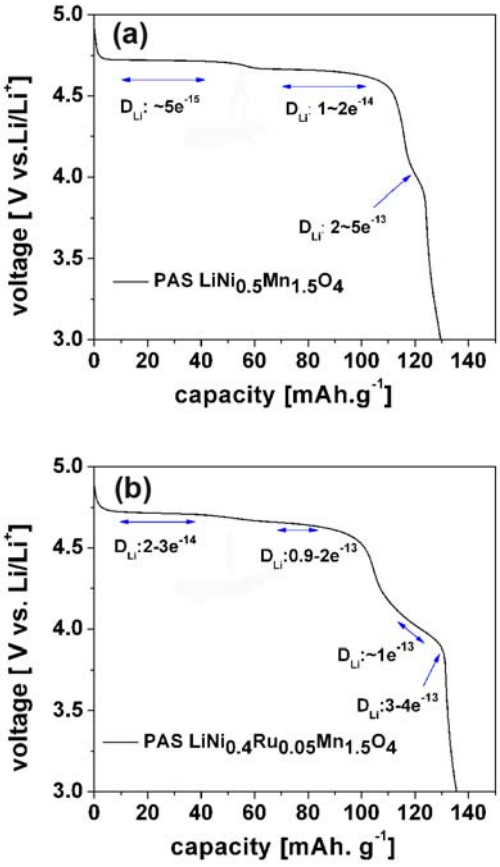

Figure 6. The calculated D_{Li} of (a) $LiNi_{0.5}Mn_{1.5}O_4$ and (b) $LiNi_{0.4}Ru_{0.05}Mn_{1.5}O_4$

To reveal the difference in lithium diffusivity within the particles of the $LiNi_{0.5}Mn_{1.5}O_4$ and the Ru doped $LiNi_{0.5}Mn_{1.5}O_4$, potential intermittent titration technique (PITT) was employed to measure the lithium diffusion coefficients (D_{Li}) of the nano sized $LiNi_{0.5}Mn_{1.5}O_4$ and $LiNi_{0.4}Ru_{0.05}Mn_{1.5}O_4$ synthesized by polymer assisted method. During the measurement, a potential drop, c.a. 10 mV, was applied and stepped to next level until the corresponded current was below ~1μA. mg^{-1}. The calculation of the D_{Li} was using the Eq. (1):

$$It^{1/2} = \frac{D^{1/2}\Delta Q}{L\pi^{1/2}} \quad (1)$$

where I and t are the current and time, respectively, D is the diffusion coefficient of lithium, ΔQ is the amount of charge injected during each potential step. L is the diffusion distance, which approximately equals to the radius of the primary spinel particles as determined by SEM images (c.a. 150 nm). Details of this method have been elucidated by Kunduraci et al.[36] and Aurbach et al.[51] The obtained PITT results in Figure 6a and 6b clearly show that in the 4.7 V plateau, D_{Li} of the $LiNi_{0.4}Ru_{0.05}Mn_{1.5}O_4$ is almost 10 times higher than that of the $LiNi_{0.5}Mn_{1.5}O_4$.

The rate capabilities of the $LiNi_{0.5-2x}Ru_xMn_{1.5}O_4$ (x=0, 0.01, 0.03 and 0.05) were assessed and shown through Figure 7a-7d.

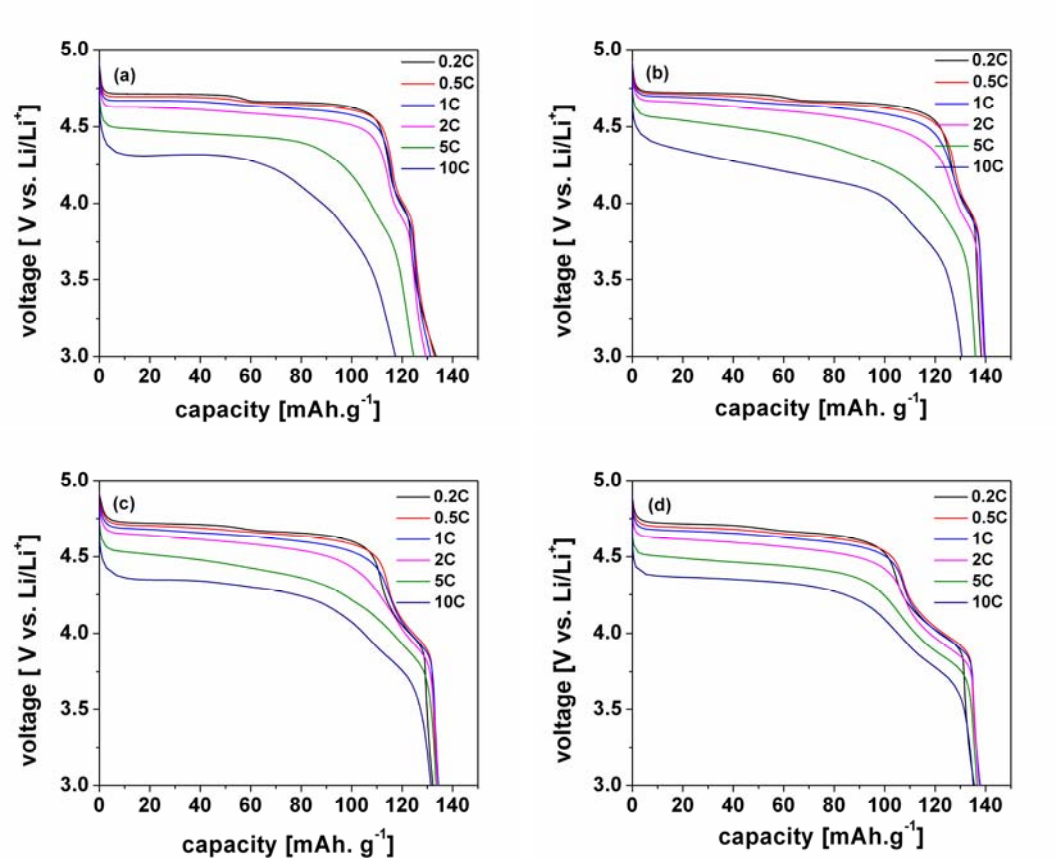

Figure 7. Rate capability of the $LiNi_{0.5-2x}Ru_xMn_{1.5}O_4$ (x=0, 0.01, 0.03 and 0.05)

As shown in Figure 7, at the low discharge current of 0.2 C, all the nano sized $LiNi_{0.5-2x}Ru_xMn_{1.5}O_4$ show the similar discharge curves as the micron sized $LiNi_{0.5-2x}Ru_xMn_{1.5}O_4$ in our previous research. The particle size effect is prominent when they are discharged at higher discharge rates. The nano sized $LiNi_{0.5}Mn_{1.5}O_4$ exhibits much smaller polarization at 5 C and 10 C compared to micron sized $LiNi_{0.5}Mn_{1.5}O_4$,[39] and a capacity of 117 mAh.g^{-1} was obtained at 10 C. With the increase of Ru doping content, the capacity of the nano sized $LiNi_{0.5-2x}Ru_xMn_{1.5}O_4$ at 10 C further increases to 130 and 135 mAh. g^{-1}, and the polarization is significantly suppressed. While the micron sized $LiNi_{0.4}Ru_{0.05}Mn_{1.5}O_4$ can only deliver 117 mAh. g^{-1} at 10 C rate. [39] It is obviously that reduction of particle size significantly improves the rate capability of Ru doped $LiNi_{0.5}Mn_{1.5}O_4$.

Table 2 compares our results of high rate capability and results of other research work. Fe doped $LiNi_{0.5}Mn_{1.5}O_4$ can release 106 mAh. g^{-1} at 10 C rate.[32] Cr doped $LiNi_{0.5}Mn_{1.5}O_4$ maximally can release near 140 mAh. g^{-1} at 10 C rate.[29] However, these results are obtained by using 20 wt% super P or carbon, which is twice the weight of our conductive agent. This will inevitably lower the power density of the battery due to low weight percentage of active material. The micron sized $LiNi_{0.4}Ru_{0.05}Mn_{1.5}O_4$ in our previous research can release 117 mAh. g^{-1} at 10 C exhibiting better performance than others metal doping results.[39] We also noticed that recently Ma et al.[52] reported that micron sized $LiNi_{0.5}Mn_{1.5}O_4$ can release nearly 130 mAh. g^{-1} at 20 C in their research work as shown in table 2. However, such

unusual high performance is only feasible when a large external pressure is applied on the cell using a C clamp, which could significantly reduce the resistance.

Nano sized $LiNi_{0.5}Mn_{1.5}O_4$ reported can maximally deliver about 85 mAh. g^{-1} at 10 C.[36] And others have only reported 5 C and 8 C discharge capacity,[35,37-38] which are also below our result at 10 C. Our nano sized $LiNi_{0.4}Ru_{0.05}Mn_{1.5}O_4$ can deliver 135 mAh. g^{-1} demonstrating that a superior rate capability of the $LiNi_{0.5}Mn_{1.5}O_4$ can be achieved through combining nanotechnology and Ru doping.

Table 2. Discharge capacity at high rate of recent research work

Cathodes	Particle size	Capacity	Remarks
$LiNi_{0.4}Ru_{0.05}Mn_{1.5}O_4$[39]	~1 μm	117 mAh. g^{-1}	10 C and 10 wt% carbon
$LiNi_{0.42}Fe_{0.08}Mn_{1.5}O_4$[32]	~1 μm	106 mAh. g^{-1}	10 C and 20 wt% carbon
$LiNi_{0.45}Cr_{0.1}Mn_{1.45}O_4$[53]	~1 μm	~40 mAh. g^{-1}	10 C and 20 wt% carbon
$LiNi_{0.4}Cr_{0.2}Mn_{1.5}O_4$[29]	~1 μm	~140 mAh. g^{-1}	10 C and 20 wt% super P
$LiNi_{0.5}Mn_{1.5}O_4$[52]	3~5 μm	~130 mAh. g^{-1}	20 C, 15 wt% carbon and external pressure on cell
$LiNi_{0.5}Mn_{1.5}O_4$[35]	70~80 nm	~105 mAh. g^{-1}	8 C and 20 wt% carbon
$LiNi_{0.5}Mn_{1.5}O_4$[36]	~70 nm	~85 mAh. g^{-1}	10 C and 13 wt% super P
$LiNi_{0.5}Mn_{1.5}O_4$[37]	~140 nm	~108 mAh. g^{-1}	5 C and 10 wt% carbon
$LiNi_{0.5}Mn_{1.5}O_4$[38]	~100 nm	~117 mAh. g^{-1}	5 C and 10 wt% carbon
$LiNi_{0.4}Ru_{0.05}Mn_{1.5}O_4$	~300 nm	135 mAh. g^{-1}	10 C and 10 wt% super P

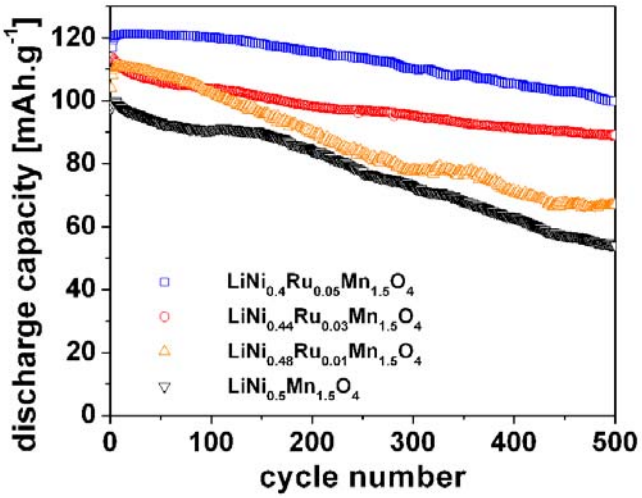

Figure 8. Cyclic performance of the the $LiNi_{0.5-2x}Ru_xMn_{1.5}O_4$ (x=0, 0.01, 0.03 and 0.05) at 10 C charge/discharge rate.

The cyclic performances of the nano sized $LiNi_{0.5-2x}Ru_xMn_{1.5}O_4$ at the 10 C charge/discharge rate were compared in Figure 8. The $LiNi_{0.5}Mn_{1.5}O_4$ shows the worst performance, with a maximum 100 mAh. g^{-1} at the beginning, and 54 mAh. g^{-1} at the last cycle (54% capacity retention). The $LiNi_{0.4}Ru_{0.05}Mn_{1.5}O_4$ exhibits the best among all samples, which can release c.a. 121 mAh. g^{-1} at the first cycles and maintains 100 mAh. g^{-1} at the 500^{th} cycle (82.6% capacity retention). It is clear to see that both the capacity retention and the available capacity at the last cycle are increased with increase in Ru doping content. While, we have shown previously that the micron sized $LiNi_{0.5}Mn_{1.5}O_4$ and $LiNi_{0.4}Ru_{0.05}Mn_{1.5}O_4$ can only release 40 mAh. g^{-1} and 93 mAh. g^{-1} at the end of 500 cycles, respectively[39]. Obviously, the high rate cyclic performance is also improved by reduction of particle size, and the nano sized $LiNi_{0.4}Ru_{0.05}Mn_{1.5}O_4$ shows best performances among them.

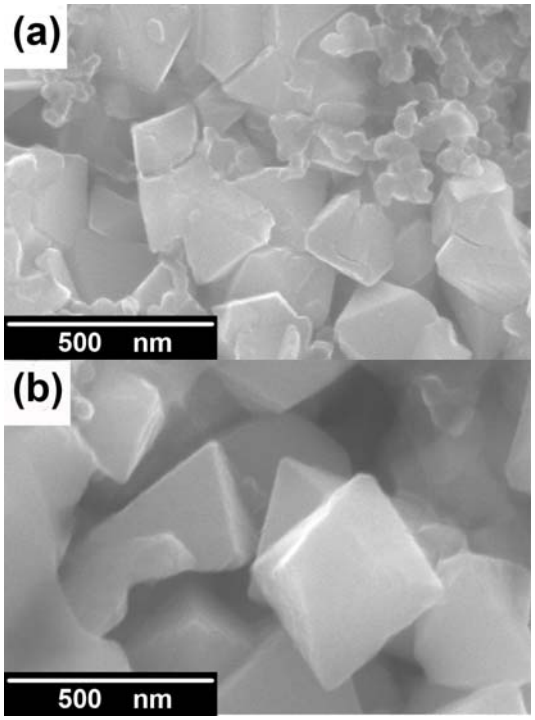

Figure 9. Particles' morphology of (a) $LiNi_{0.5}Mn_{1.5}O_4$ and (b) $LiNi_{0.4}Ru_{0.05}Mn_{1.5}O_4$ after 500 cycles at 10 C charge/discharge rate.

The cyclic performance is mainly affected by the structural stability. As described in introduction, at the end of high-rate discharge, Li^+ ions are easily segregated at the surface of the $LiNi_{0.5}Mn_{1.5}O_4$ due to limited lithium ion transportation ability, hence resulting in a large amount of Mn^{3+} ions on the surfaces causing severe J-T distortion and detrimental reaction with electrolyte to damage particles. The result of PITT tests has shown that the $LiNi_{0.4}Ru_{0.05}Mn_{1.5}O_4$ possesses much higher lithium diffusivity than the $LiNi_{0.5}Mn_{1.5}O_4$, therefore, the $LiNi_{0.4}Ru_{0.05}Mn_{1.5}O_4$ will receive much less attack caused by Mn^{3+} than the $LiNi_{0.5}Mn_{1.5}O_4$, and the particles of the $LiNi_{0.4}Ru_{0.05}Mn_{1.5}O_4$ would show better integrity than those of the $LiNi_{0.5}Mn_{1.5}O_4$. To verify this, particles' morphologies of both nano sized $LiNi_{0.5}Mn_{1.5}O_4$ and nano

sized $LiNi_{0.4}Ru_{0.05}Mn_{1.5}O_4$ after the high-rate cyclic test were examined by SEM and exhibited in Figure 9.

Figure 9a provides clear evidence of damage on the nano particles of the $LiNi_{0.5}Mn_{1.5}O_4$. It can be seen that there are many cracks appearing on particles of the $LiNi_{0.5}Mn_{1.5}O_4$, and some particles are even broken, while the nano particles of the $LiNi_{0.4}Ru_{0.05}Mn_{1.5}O_4$ shown in Figure 9b maintain their original morphology and no distinct crack appears. The tiny particles with an average size of 50 nm shown in Figure 9 are Super P. The faster charge transportation ability of $LiNi_{0.4}Ru_{0.05}Mn_{1.5}O_4$ resulting from both the reduced particles' size and Ru doping effectively prevents the present of undesirable Mn^{3+} ions. Therefore, the best 10 C cyclic performance achieved on nano sized $LiNi_{0.4}Ru_{0.05}Mn_{1.5}O_4$ can be explained by its capability of suppressing polarization and maintaining crystal structure stability.

To further examine the high rate cyclic performance of the nano sized $LiNi_{0.4}Ru_{0.05}Mn_{1.5}O_4$, 1000 cycles 10 C charge/discharge test was performed and the result is shown in Figure 10. It can be seen that initially the $LiNi_{0.4}Ru_{0.05}Mn_{1.5}O_4$ can release nearly 120 mAh. g^{-1}, and after 1000 cycles, it still can release 77 mAh. g^{-1} (capacity retention 65%). Such long term high rate cyclic performance has not been reported by other researchers.

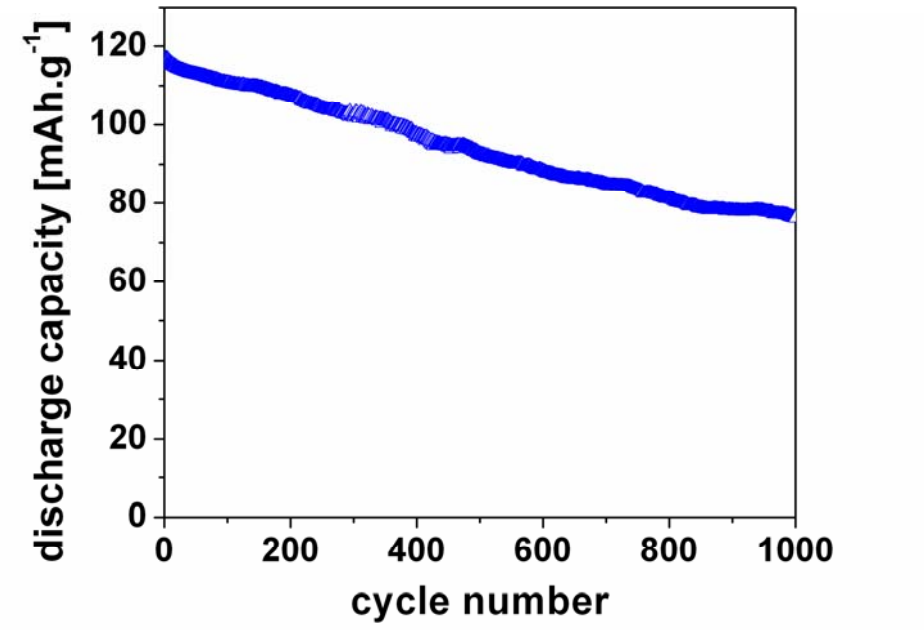

Figure 10. 1000 cycles performance of the $LiNi_{0.4}Ru_{0.05}Mn_{1.5}O_4$ at 10 C charge/discharge rate.

4. Conclusion

Nano sized $LiNi_{0.5-2x}Ru_xMn_{1.5}O_4$ (x=0, 0.01, 0.03 and 0.05) spinels have been successfully synthesized by polymer assisted method. SEM observation shows that particles' sizes of $LiNi_{0.5-2x}Ru_xMn_{1.5}O_4$ are around 300 nm. XRD and FTIR measurements prove that all Ru doped samples have phase pure spinel structure with $Fd\bar{3}m$ space group, while pristine $LiNi_{0.5}Mn_{1.5}O_4$ contains impurity phase ($Li_xNi_{1-x}O$). The nano sized $LiNi_{0.5}Mn_{1.5}O_4$ can release 117 mAh. g^{-1} at 10 C discharge rate; while, the nano sized $LiNi_{0.4}Ru_{0.05}Mn_{1.5}O_4$ can deliver 135 mAh. g^{-1} at 10 C discharge rate. In 500 cycles 10 C charge/discharge test, the nano sized $LiNi_{0.4}Ru_{0.05}Mn_{1.5}O_4$ can initially deliver near 121 mAh. g^{-1} and still keep 100 mAh. g^{-1} at the 500^{th} cycle

exhibiting much better cyclic performance than the pristine $LiNi_{0.5}Mn_{1.5}O_4$. It also exhibits excellent cyclic performances when charge/discharged at 10C for 1000 cycles. The great improvements on high rate performances of Ru doped cathodes can be attributed to their higher electronic conductivity and lithium diffusion coefficient, which are achieved through both Ru doping and reduction of particle size.

Acknowledgements

This research is supported by AFOSR/AOARD RD through the grant FA2386-10-1-4013 managed by Dr. Rengasamy Ponnappan.

We gratefully thank Dr. Ponnappan for useful discussions. Assistances from Mr. P.F. Xiao and Dr. H. Xia are appreciated. We also acknowledge Changzhou Timcal Graphite Corp. Ltd for the support in providing Super P.

References

(1) Tarascon, J. M.; Armand, M. *Nature* **2001**, *414*, 359.
(2) Goodenough, J. B. *Journal of Power Sources* **2007**, *174*, 996.
(3) Kikkawa, J.; Akita, T.; Hosono, E.; Zhou, H. S.; Kohyama, M. *Journal of Physical Chemistry C* **2010**, *114*, 18358.
(4) Fergus, J. W. *Journal of Power Sources* **2010**, *195*, 939.
(5) Saravanan, K.; Reddy, M. V.; Balaya, P.; Gong, H.; Chowdari, B. V. R.; Vittal, J. J. *Journal of Materials Chemistry* **2009**, *19*, 605.
(6) Liddle, B. J.; Collins, S. M.; Bartlett, B. M. *Energy & Environmental Science* **2010**.
(7) Yamaguchi, H.; Yamada, A.; Uwe, H. *Physical Review B* **1998**, *58*, 8.
(8) Amatucci, G. G.; Pereira, N.; Zheng, T.; Tarascon, J. M. *Journal of the Electrochemical Society* **2001**, *148*, A171.
(9) Amatucci, G.; Du Pasquier, A.; Blyr, A.; Zheng, T.; Tarascon, J. M. *Electrochimica Acta* **1999**, *45*, 255.
(10) Capsoni, D.; Bini, M.; Chiodelli, G.; Massarotti, V.; Azzoni, C. B.; Mozzati, M. C.; Comin, A. *Physical Chemistry Chemical Physics* **2001**, *3*, 2162.
(11) Sanchez, L.; Tirado, J. L. *Journal of the Electrochemical Society* **1997**, *144*, 1939.
(12) Ohzuku, T.; Kitano, S.; Iwanaga, M.; Matsuno, H.; Ueda, R. In *8th International*

Meeting on Lithium Batteries Nagoya, Japan, 1996, p 646.
(13) Tarascon, J. M.; McKinnon, W. R.; Coowar, F.; Bowmer, T. N.; Amatucci, G.; Guyomard, D. *Journal of the Electrochemical Society* **1994**, *141*, 1421.
(14) Yamada, A. *Journal of Solid State Chemistry* **1996**, *122*, 160.
(15) Robertson, A. D.; Lu, S. H.; Howard, W. F. *Journal of the Electrochemical Society* **1997**, *144*, 3505.
(16) Gummow, R. J.; Dekock, A.; Thackeray, M. M. *Solid State Ionics* **1994**, *69*, 59.
(17) Zhong, Q. M.; Bonakdarpour, A.; Zhang, M. J.; Gao, Y.; Dahn, J. R. *Journal of the Electrochemical Society* **1997**, *144*, 205.
(18) Ariyoshi, K.; Iwakoshi, Y.; Nakayama, N.; Ohzuku, T. *Journal of the Electrochemical Society* **2004**, *151*, A296.
(19) Santhanam, R.; Rambabu, B. *Journal of Power Sources* **2010**, *195*, 5442.
(20) Arunkumar, T. A.; Manthiram, A. *Electrochemical and Solid-State Letters* **2005**, *8*, A403.
(21) Kim, J. H.; Myung, S. T.; Yoon, C. S.; Kang, S. G.; Sun, Y. K. *Chemistry of Materials* **2004**, *16*, 906.
(22) Liu, G. Q.; Wen, L.; Liu, Y. M. *Journal of Solid State Electrochemistry* **2010**, *14*, 2191.
(23) Myung, S. T.; Komaba, S.; Kumagai, N.; Yashiro, H.; Chung, H. T.; Cho, T. H. *Electrochimica Acta* **2002**, *47*, 2543.
(24) Mohamedi, M.; Makino, A.; Dokko, K.; Itoh, T.; Uchida, I. *Electrochimica Acta* **2002**, *48*, 79.
(25) Sun, Y. K.; Yoon, C. S.; Oh, I. H. *Electrochimica Acta* **2003**, *48*, 503.
(26) Fan, Y. K.; Wang, J. M.; Tang, Z.; He, W. C.; Zhang, J. Q. *Electrochimica Acta* **2007**, *52*, 3870.
(27) Liu, J.; Manthiram, A. *Journal of the Electrochemical Society* **2009**, *156*, A833.
(28) Yi, T. F.; Li, C. Y.; Zhu, Y. R.; Shu, J.; Zhu, R. S. *Journal of Solid State Electrochemistry* **2009**, *13*, 913.
(29) Aklalouch, M.; Amarilla, J. M.; Rojas, R. M.; Saadoune, I.; Rojo, J. M. *Electrochemistry Communications* **2010**, *12*, 548.
(30) Ein-Eli, Y.; Vaughey, J. T.; Thackeray, M. M.; Mukerjee, S.; Yang, X. Q.; McBreen, J. *Journal of the Electrochemical Society* **1999**, *146*, 908.
(31) Ito, A.; Li, D.; Lee, Y.; Kobayakawa, K.; Sato, Y. *Journal of Power Sources* **2008**, *185*, 1429.
(32) Liu, J.; Manthiram, A. *Journal of Physical Chemistry C* **2009**, *113*, 15073.
(33) Liu, G. Q.; Wen, L.; Liu, G. Y.; Tian, Y. W. *Journal of Alloys and Compounds* **2010**, *501*, 233.
(34) Schalkwijk, W. A. v.; Scrosati, B. *Advances in lithium-ion batteries*; Kluwer Academic/Plenum Publishers: New York, NY, 2002.
(35) Arrebola, J. C.; Caballero, A.; Cruz, M.; Hernan, L.; Morales, J.; Castellon, E. R. *Advanced Functional Materials* **2006**, *16*, 1904.
(36) Kunduraci, M.; Amatucci, G. G. *Electrochimica Acta* **2008**, *53*, 4193.
(37) Gao, J. A.; Li, J. A. J.; Jiang, C. Y.; Wan, C. R. *Journal of the Electrochemical Society* **2010**, *157*, A899.

(38) Zhang, X. F.; Liu, J.; Yu, H. Y.; Yang, G. L.; Wang, J. W.; Yu, Z. J.; Xie, H. M.; Wang, R. S. *Electrochimica Acta* **2010**, *55*, 2414.
(39) Wang, H. L.; Xia, H.; Lai, M. O.; Lu, L. *Electrochemistry Communications* **2009**, *11*, 1539.
(40) Le, M. L. P.; Strobel, P.; Alloin, F.; Pagnier, T. *Electrochimica Acta* **2010**, *56*, 592.
(41) Matsumoto, H.; Murakami, D.; Shimura, T.; Hashimoto, S. I.; Iwahara, H. *Journal of Electroceramics* **2001**, *7*, 107.
(42) Krutzsch, B.; Mossner, B.; Kemmlersack, S. *Journal of the Less-Common Metals* **1986**, *118*, 123.
(43) Johannes, M. D.; Stux, A. M.; Swider-Lyons, K. E. *Physical Review B* **2008**, *77*.
(44) Balaya, P.; Li, H.; Kienle, L.; Maier, J. *Advanced Functional Materials* **2003**, *13*, 621.
(45) Shannon, R. D. *Acta Crystallographica Section A* **1976**, *32*, 751.
(46) Amine, K.; Tukamoto, H.; Yasuda, H.; Fujita, Y. In *8th International Meeting on Lithium Batteries* Nagoya, Japan, 1996, p 604.
(47) Wei, Y. J.; Kim, K. B.; Chen, G. *Electrochimica Acta* **2006**, *51*, 6599.
(48) Alcantara, R.; Jaraba, M.; Lavela, P.; Tirado, J. L.; Zhecheva, E.; Stoyanova, R. *Chemistry of Materials* **2004**, *16*, 1573.
(49) Reddy, M. V.; Manoharan, S. S.; John, J.; Singh, B.; Rao, G. V. S.; Chowdari, B. V. R. *Journal of the Electrochemical Society* **2009**, *156*, A652.
(50) Ooms, F. G. B.; Kelder, E. M.; Schoonman, J.; Wagemaker, M.; Mulder, F. M. *Solid State Ionics* **2002**, *152*, 143.
(51) Levi, M. D.; Levi, E. A.; Aurbach, D. *Journal of Electroanalytical Chemistry* **1997**, *421*, 89.
(52) Ma, X. H.; Kang, B.; Ceder, G. *Journal of the Electrochemical Society* **2010**, *157*, A925.
(53) Liu, D. Q.; Lu, Y. H.; Goodenough, J. B. *Journal of the Electrochemical Society* **2010**, *157*, A1269.